

The Canis Major Star Forming Region

Jane Gregorio-Hetem

Universidade de São Paulo
Rua do Matão, 1226 - IAG/USP, 05508-900, São Paulo, SP, Brazil

Abstract. The shape of the main arc formed by the Canis Major clouds has been suggested to result from a supernova explosion possibly triggering the recent star formation activity. The presence of dozens of OB stars and reflection nebulae forms the CMa OB1/R1 associations. More than a hundred emission line stars are found in this region, including the famous Z CMa, a binary system containing a Herbig Be star and a FUor companion. Several embedded infrared clusters with different ages are associated with the CMa clouds. The main characteristics of the region in terms of cloud structure, stellar content, age of associated young clusters, distance, and X-ray emission are presented in this chapter. Some of the arguments in favor and against the hypothesis of induced star formation are discussed in the last section.

1. The Canis Major Associations

The star-forming region in Canis Major is characterized by a concentrated group of early type stars, which was first identified as a stellar association by Ambartsumian (1947). The angular size of 4° in diameter was defined by Markarian (1952), who estimated a distance of 960 pc, based on the identification of 11 probable members.

Ruprecht (1966) established the approximate boundaries: $222^\circ < l < 226^\circ$ and $-3.4^\circ < b < +0.7^\circ$ of the CMa OB1 association. He suggested that NGC 2353, a young cluster of age ~ 12.6 Myr (Hoag et al. 1961) and with a distance of ~ 1315 pc (Becker 1963), constitutes the main stellar concentration of CMa OB1. More recently, Fitzgerald et al. (1990) estimated an age of 76 Myr for NGC 2353 and a distance of 1.2 kpc, indicating that the cluster is unrelated to CMa OB1 despite their similar distances.

Clariá (1974a,b) studied the space distribution of O and B stars, based on UBV photometry obtained for 247 stars. The estimated $E(B-V)$ color excess confirms the existence of a group of young OB stars together with excited gas and obscuring matter, which belong to the CMa OB1 association. Clariá used these data to derive a distance of 1.15 kpc and an age of 3 Myr.

The CMa R1 association is defined by a group of stars embedded in reflection nebulae located within the boundaries of the OB1 association. It was first identified by van den Bergh (1966), who listed ten stars distributed in the $-3.4^\circ < b < -2^\circ$ range. Racine (1968) reported photometric and spectroscopic observations of the CMa R1 members and suggested that the reflection nebulae seem to be nearer than the CMa OB1 association. Clariá (1974b) compares the distance moduli that he obtained with those values estimated by Racine. The evaluation of the discrepancies led to the conclusion of the physical relation of the CMa OB1/R1 associations.



Figure 1. The interface between the HII region and the neutral gas forms a north-south oriented ridge in the CMa R1 association. The round compact emission structure with a dark lane to the upper right is IC 2177. Courtesy John P. Gleason.

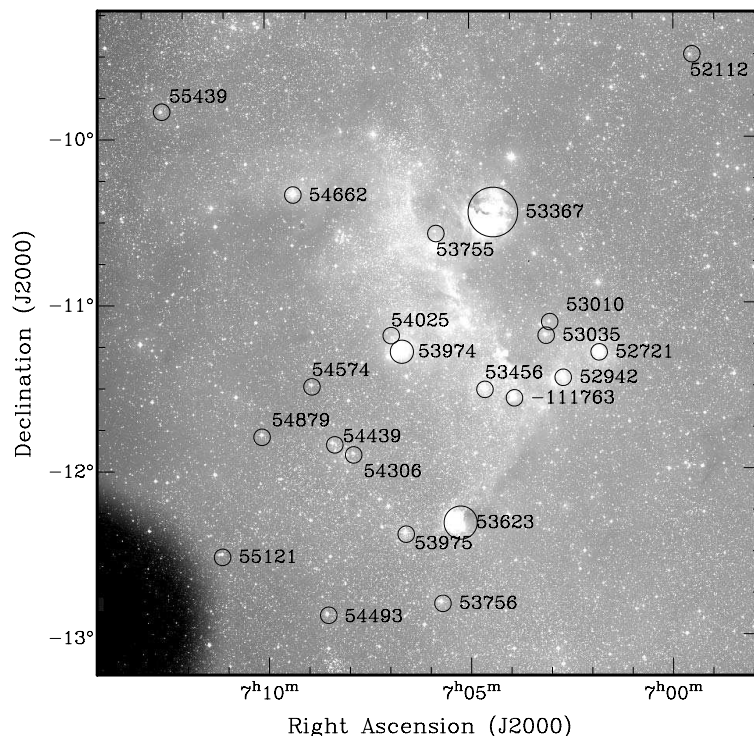


Figure 2. Optical image of CMA R1 obtained from the Digitized Sky Survey - DSS 2 in the R band (the dark-spot in the lower-right corner is an artifact). Some of the members are identified by their HD/BD numbers.

More than 30 nebulae (Herbst, Racine, & Warner 1978) are found in the CMA OB1 association, in particular three connected HII regions S292, S296 and S297 (Sharpless 1959). Two of the conspicuous features are the long arc of emission nebulosity S296 and the nearly circular nebulosity IC 2177 surrounding the Be star HD 53367. The members of the CMA OB1/R1 association are listed in Table 1. Figures 1 and 2 present optical images of the entire region. Schematic maps showing early-type stars, clusters, emission and reflection nebulae, and dark clouds are presented in Figures 3 and 4. Other associations or stellar clusters are found between $l \sim 233^\circ$ to 237° and $b \sim -6^\circ$ to -11° (not identifiable in the figures of this chapter). Kopylov (1958) denoted this region as CMA II, or CMA OB2 in current nomenclature. Eggen (1981) reported observations of 135 stars, which are members of the clusters NGC 2287 and Cr 121 (Collinder 1931). The distances derived from the photometric data are 704 pc and 1.17 kpc, respectively. The age determination indicates that NGC 2287 (100 Myr) is considerably older than Cr 121 (1.5 Myr).

Table 1.: Members of CMa OB1/R1 presented by C74 (Clariá 1974b) and/or SEI99 (Shevchenko et al. 1999). The list gives Galactic (l , b) and equatorial (J2000) coordinates; visual magnitude and spectral type. Other cross identification names and related nebulae are also provided, when available - HRW (Herbst, Racine, & Warner 1978); vdB (van den Bergh 1966) in the last column and Notes.

C74	SEI 99	HD/BD	l , b	RA (J2000)	DEC (J2000)	V (mag)	ST	
13		51361	225.15, -4.81	6 56 30.3	-13 03 33	10.1	B9Ib	
18		51454	223.32, -3.73	6 57 04.1	-10 56 50	9.4	B8IV	
20		51479	222.74, -3.42	6 57 07.9	-10 16 47	8.4	B7V	a
24		51542	223.51, -3.75	6 57 21.2	-11 07 03	9.6	B3V	
32		51785	222.00, -2.69	6 58 23.6	-09 17 44	9.5	B6V	
39		51961	223.48, -3.28	6 59 00.4	-10 52 55	9.6		
46		52112	222.32, -2.53	6 59 35.3	-09 30 04	8.8	B3V	
48		52159	223.81, -3.25	6 59 42.6	-11 09 26	9.6	B5Vne	
	7		223.58, -2.96	7 00 20.6	-10 49 14	11.4	A8-F0	
	11		223.64, -2.95	7 00 28.7	-10 52 12	10.2	B9	
	9		224.39, -3.32	7 00 32.1	-11 42 26	11.9	B6	
	19		223.64, -2.91	7 00 38.0	-10 51 27	11.3	B7-8	
	18	52412	224.24, -3.22	7 00 38.5	-11 31 45	10.2	B4-6	
	16		224.85, -3.53	7 00 38.5	-12 12 39	11.3	A0	
	20		223.66, -2.92	7 00 38.6	-10 52 34	11.6	B9	
	21		223.40, -2.78	7 00 38.8	-10 34 45	11.6	B8-9	
	23		223.74, -2.93	7 00 44.7	-10 57 24	11.3	B5-6	
	25		224.18, -3.05	7 01 07.8	-11 24 05	10.8	A1-2	
	28		223.89, -2.87	7 01 14.9	-11 03 48	10.0	B3	
	30		223.67, -2.72	7 01 22.9	-10 47 42	10.9	B8	
63	158	52721	224.17, -2.85	7 01 49.5	-11 18 03	6.6	B2Vne	b
	38		224.21, -2.87	7 01 49.6	-11 20 39	11.7		c
	40	52746	224.97, -3.23	7 01 58.0	-12 10 51	9.75	B6	
	45		223.26, -2.32	7 02 04.9	-10 14 37	11.0	B9	
	50		223.29, -2.30	7 02 11.1	-10 15 49	10.5	B3	
	52		224.70, -2.97	7 02 23.7	-11 49 40	11.1	B8-9	
	58		223.72, -2.43	7 02 31.4	-10 42 43	10.2	B9	
	57		224.80, -2.95	7 02 37.9	-11 54 03	11.1	B7-8	
	56	-121748	225.09, -3.11	7 02 38.4	-12 13 59	10.3	B8	d
	160		224.39, -2.73	7 02 42.3	-11 26 10	11.9	Ae	e
67	159	52942	224.41, -2.73	7 02 42.6	-11 27 11	8.1	B2.5IV	f
	66	53011	224.89, -2.91	7 02 57.7	-11 58 10	10.1	B7-9	
70	68		224.44, -2.68	7 02 58.4	-11 27 24	11.2	B2	g
71	70	53010	224.14, -2.51	7 03 02.3	-11 07 01	8.9	B2.5V	
	71		224.62, -2.73	7 03 06.8	-11 38 29	13.1		
72	72	53035	224.23, -2.52	7 03 07.8	-11 11 57	7.9	B1	
	73		224.63, -2.72	7 03 10.6	-11 38 27	10.6	B3	h
	77		224.42, -2.57	7 03 19.4	-11 23 27	11.7	B3	
	78		224.01, -2.36	7 03 20.5	-10 55 53	10.9	B2	
75	79	-101839	223.82, -2.24	7 03 24.6	-10 42 16	9.7	B3V	i

Continued on Next Page...

(a) vdB 86; (b) GU CMa, HRW 2, vdB 88; (c) HRW 3; (d) HRW 4, vdB 89; (e) HT CMa, LkHa 218; (f) FZ CMa, HRW 5, vdB 90a, S 295; (g) HRW 6; (h) HRW 7; (i) HRW 8, vdB 91; (j) ALS137; (k) Z CMa, HRW 9; (l) HRW 12, vdB 92c; (m) HRW 13, vdB 92b; (n) HRW 11, vdB 92a; (o) HRW 15; (p) HU CMa, LkHa 220; (q) HRW 16; (r) HRW 17; (s) HRW 18; (t) HRW 19; (u) IC 2177, HRW 20, S 292, L 1657; (v) HRW 23; (w) HRW 24; (x) HRW 25; (y) HRW 26; (z) HRW 27, vdB 94; (aa) HRW 28; (bb) FM CMa; (cc) FN CMa, HRW 29, vdB 95;

Table 1.: Members of CMa OB1/R1 (continued)

C74	SEI 99	HD/BD	l, b	RA (J2000)	DEC (J2000)	V (mag)	ST	
	80		224.77, -2.68	7 03 34.6	-11 44 55	10.6	B0	j
	86		223.61, -2.06	7 03 39.3	-10 26 13	11.5	B9-A0	
	82		224.58, -2.56	7 03 39.3	-11 31 51	11.6	B8	
	81		224.84, -2.70	7 03 39.4	-11 49 35	10.5	B9	
	84		224.46, -2.49	7 03 40.4	-11 23 31	11.9	A	
76	161	53179	224.54, -2.52	7 03 43.2	-11 33 06	9.9	Bpe	k
	88		224.55, -2.50	7 03 49.6	-11 28 23	11.6		
77	92	-111762	224.56, -2.48	7 03 54.4	-11 28 29	10.0	B2	l
	93		224.64, -2.52	7 03 54.6	-11 33 40	10.1		
78	91	-111763	224.65, -2.53	7 03 54.9	-11 34 34	8.9	B1.5V	m
79	89	-111761	224.65, -2.52	7 03 55.0	-11 34 30	9.3	B2	n
14	94		224.65, -2.52	7 03 56.4	-11 34 39	12.1		
	95		224.67, -2.52	7 03 58.5	-11 35 30	11.3		
17	97		224.32, -2.34	7 03 59.0	-11 11 58	10.4	B5	o
	101		224.15, -2.24	7 04 00.7	-11 00 03	11.2	B6-8	
	99		224.53, -2.43	7 04 02.3	-11 25 39	10.5	B3-5	
	100		224.63, -2.48	7 04 02.6	-11 32 15	11.7	B8-9	
	102		224.54, -2.43	7 04 03.9	-11 26 10	9.93		
	103	-11 1765	224.59, -2.44	7 04 05.4	-11 28 56	10.3	B2	
	162		224.55, -2.42	7 04 06.8	-11 26 09	11.8	B5e	p
81	107		224.44, -2.36	7 04 06.9	-11 18 49	11.0	B6	q
	108		225.21, -2.73	7 04 12.5	-12 10 19	11.1	B6-8	
	111		224.45, -2.34	7 04 13.0	-11 19 01	11.8	B8	r
84	114	53339	224.53, -2.37	7 04 15.9	-11 24 05	9.4	B3V	
	112	53396	224.82, -2.51	7 04 17.4	-11 43 10	10.7	B9	
	116		224.45, -2.32	7 04 17.4	-11 18 09	12.0	A1	s
	117		224.44, -2.31	7 04 19.0	-11 17 13	12.1	A0	t
	119		224.77, -2.46	7 04 21.7	-11 39 05	10.7	B5	
86	163	53367	223.71, -1.90	7 04 25.5	-10 27 16	7	B0IVe	u
	121		224.68, -2.39	7 04 26.1	-11 32 20	12.3	B8	
	123		224.71, -2.39	7 04 30.6	-11 33 52	11.8	B5-7	
	124		224.88, -2.46	7 04 34.9	-11 44 57	10.5	B7	
92	164	53456	224.68, -2.34	7 04 38.3	-11 31 27	7.3	B0V	
90	125	53457	225.10, -2.55	7 04 38.5	-11 59 08	9.3	B6-7	
	127		225.48, -2.73	7 04 44.1	-12 24 32	10.8	B6	
	130		223.85, -1.88	7 04 45.3	-10 34 12	10.8	B8III/IV	v
	131		224.18, -2.04	7 04 47.4	-10 56 18	13.3		w
	129		224.33, -2.12	7 04 47.5	-11 06 37	13.2		x
	132		224.47, -2.17	7 04 53.5	-11 15 19	11.7	B6-7	
	135		223.93, -1.88	7 04 54.1	-10 38 50	12.4	A1 IV	y
	137		223.70, -1.73	7 05 02.1	-10 22 04	11.4	B6-8	
	139		223.71, -1.72	7 05 04.5	-10 22 33	11.9	B9-A0	
	140	53569	224.12, -1.92	7 05 07.2	-10 50 01	10.4	B9	
	141		224.14, -1.93	7 05 07.5	-10 51 19	9.8	B9	

Continued on Next Page...

(a) vdB 86; (b) GU CMa, HRW 2, vdB 88; (c) HRW 3; (d) HRW 4, vdB 89; (e) HT CMa, LkHa 218; (f) FZ CMa, HRW 5, vdB 90a, S 295; (g) HRW 6; (h) HRW 7; (i) HRW 8, vdB 91; (j) ALS137; (k) Z CMa, HRW 9; (l) HRW 12, vdB 92c; (m) HRW 13, vdB 92b; (n) HRW 11, vdB 92a; (o) HRW 15; (p) HU CMa, LkHa 220; (q) HRW 16; (r) HRW 17; (s) HRW 18; (t) HRW 19; (u) IC 2177, HRW 20, S 292, L 1657; (v) HRW 23; (w) HRW 24; (x) HRW 25; (y) HRW 26; (z) HRW 27, vdB 94; (aa) HRW 28; (bb) FM CMa; (cc) FN CMa, HRW 29, vdB 95;

Table 1.: Members of CMa OB1/R1 (continued)

C74	SEI 99	HD/BD	l, b	RA (J2000)	DEC (J2000)	V (mag)	ST	
96		53595	224.37, -2.03	7 05 11.8	-11 06 02	9.2	B5Vn	
97	142	53623	225.47, -2.57	7 05 16.8	-12 19 34	8	B1 II/III	z
98	144	53622	224.55, -2.09	7 05 18.5	-11 17 22	9.4	B5V	
	143		224.84, -2.24	7 05 18.8	-11 36 49	10.5	B6-8	
	145		224.48, -2.02	7 05 26.4	-11 11 22	11.5	B7-8	
	146		223.70, -1.58	7 05 34.0	-10 18 17	10.9	B8-9	
100		53667	222.31, -0.85	7 05 35.2	-08 43 44	7.8	B0.5III	
101	149	53691	224.47, -1.96	7 05 37.6	-11 09 26	9.4	B3V	aa
102		53756	225.95, -2.70	7 05 42.1	-12 48 43	7.3	B2/B3II	bb
104	165	53755	223.98, -1.65	7 05 49.6	-10 34 57	6.5	B0.5V	
	156	-10 1866	224.18, -1.73	7 05 53.9	-10 47 43	10.4	B4-6	
114		53948	225.94, -2.46	7 06 33.6	-12 41 53	9.8	B5	
115		53975	225.68, -2.32	7 06 36.0	-12 23 38	6.5	B7Iab/Ib	
116		53974	224.71, -1.79	7 06 40.8	-11 17 38	5.4	B0.5IV	cc
120		54025	224.77, -1.75	7 06 56.4	-11 19 38	7.7	B1V	
131		54306	225.40, -1.82	7 07 52.9	-11 54 50	8.7	B2V	
133		54439	225.40, -1.68	7 08 23.2	-11 51 09	7.2	B2III	
134		54493	226.33, -2.12	7 08 32.2	-12 53 09	7.2	B2IV	
145		54672	240.45, -9.21	7 08 33.7	-28 36 47	7.5	F7V	
138		54574	225.14, -1.41	7 08 53.9	-11 30 05	8.8	B2V	
141		54662	224.17, -0.78	7 09 20.3	-10 20 48	6.2	O7III	
150		54879	225.55, -1.28	7 10 08.1	-11 48 10	7.7	O9.5V	
160		55096	232.97, -4.94	7 10 44.5	-20 03 56	9.5	A1IV/V	
161		55121	226.30, -1.39	7 11 08.0	-12 31 22	8.6	B3II/III	
167		55266	224.96, -0.51	7 11 46.5	-10 55 21	10	B5V	
177		55442	226.16, -0.95	7 12 29.3	-12 11 42	9.5	B3V	
178		55439	224.09, 0.16	7 12 34.8	-09 50 42	8.6	B2Ve	
184		55562	226.58, -1.03	7 12 58.1	-12 36 21	9.0	B3V	
190		55776	224.53, 0.33	7 14 01.2	-10 09 03	10.0	B8V	

(a) vdB 86; (b) GU CMa, HRW 2, vdB 88; (c) HRW 3; (d) HRW 4, vdB 89; (e) HT CMa, LkHa 218; (f) FZ CMa, HRW 5, vdB 90a, S 295; (g) HRW 6; (h) HRW 7; (i) HRW 8, vdB 91; (j) ALS137; (k) Z CMa, HRW 9; (l) HRW 12, vdB 92c; (m) HRW 13, vdB 92b; (n) HRW 11, vdB 92a; (o) HRW 15; (p) HU CMa, LkHa 220; (q) HRW 16; (r) HRW 17; (s) HRW 18; (t) HRW 19; (u) IC 2177, HRW 20, S 292, L 1657; (v) HRW 23; (w) HRW 24; (x) HRW 25; (y) HRW 26; (z) HRW 27, vdB 94; (aa) HRW 28; (bb) FM CMa; (cc) FN CMa, HRW 29, vdB 95;

Eggen (1981) proposed that stars in the Cr 121 region form two groups. The nearer concentration of stars located mainly within a 2° circle centered on $(\alpha, \delta)_{J2000} = (6^h 54^m, -23^\circ 37.5')$ is probably related to NGC 2287, because they have similar age and motion. He suggested that this is a separate association, CMa OB2.

The similarities in age and distance of Cr 121 and CMa OB1 points to a physical relation leading Eggen to argue that the Cr 121 cluster is probably an extension of CMa OB1. On the other hand, de Zeeuw et al. (1999) used *Hipparcos* data to identify Cr 121 as a moving group not related with CMa OB1. The controversy on the nature of Cr 121 is discussed further in Sect. 4.

CMa R1 contains several OB stars associated with the ring of emission nebulae coinciding with an expanding HI shell that is suggested to be a supernova remnant (SNR)

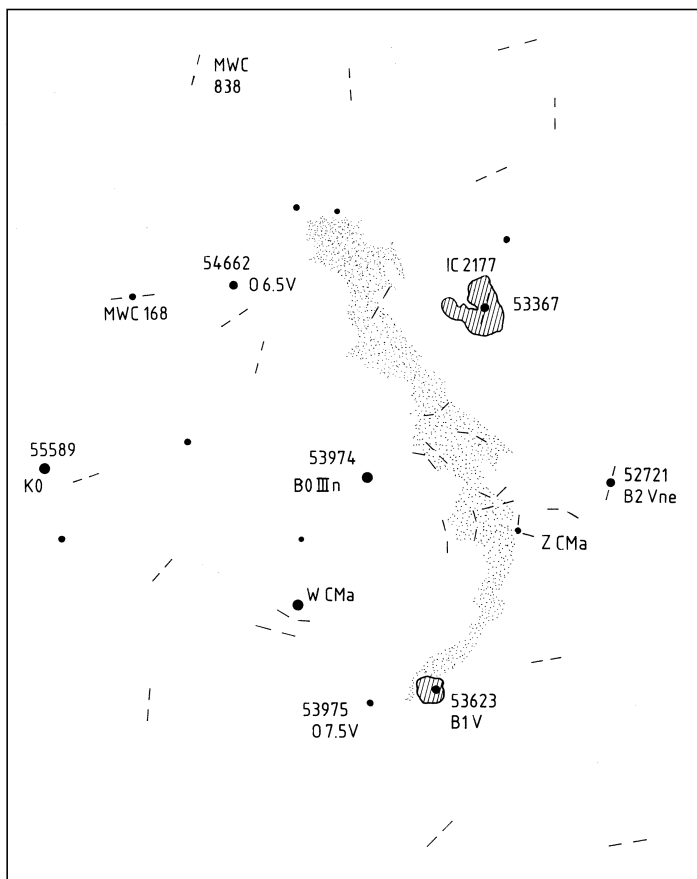


Figure 3. Schema extracted from Herbig (1991) showing the identification of early-type stars (by their HD numbers) and reflection nebulae. The marks show the positions of emission-line stars found by Wiramihardja et al. (1986). The field covers 4.1×3.3 square degrees. North is up and East is to the left.

inducing the star formation in this region (Herbst & Assousa 1977). Linear polarization observations are consistent with a model of compression by a supernova shock (Vrba, Baierlein, & Herbst 1987) but stellar winds could also produce a similar structure and morphology. A more detailed discussion on the hypothesis of star formation in CMa R1 induced by SNR is presented in Sect. 7.

2. Cloud Structure

2.1. Dust Distribution and Visual Extinction

A picture of the dust distribution of the Canis Majoris cloud complex is given in Figure 5, which shows the IRAS contours at $100 \mu\text{m}$ superposed on a DSS optical image. The higher levels of far-infrared emission are associated to emission or reflection nebulae, mainly around the stars HD 53367 (IC 2177), GU CMa, Z CMa, and HD 53623. The overall contours show the correlation of gas and dust distributions.

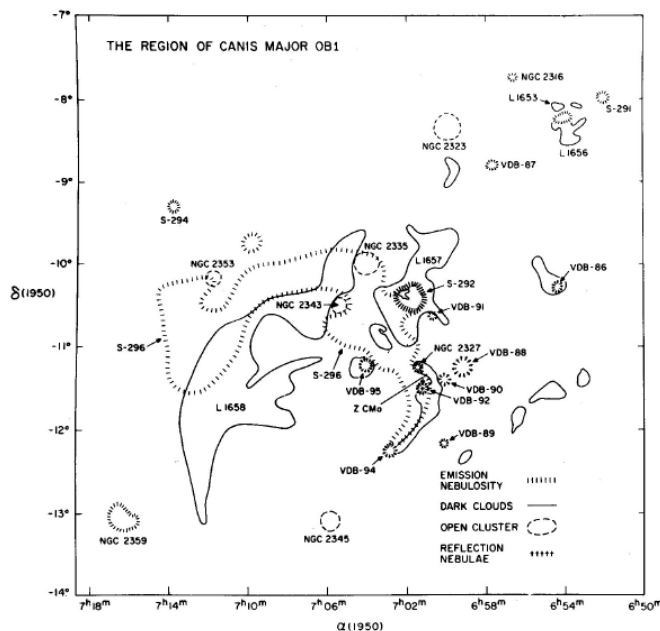


Figure 4. The distribution of the conspicuous objects found in CMa OB1/R1 region. Two dark clouds, L1658 and L1657, correspond to the main structures detected in the map of integrated ^{12}CO emission obtained by Blitz (1980). This drawing is extracted from Fig. 8 in the paper by Blitz (1980).

Figure 6 presents the CMa cloud distribution extracted from the atlas of dark clouds by Dobashi et al. (2005) and shows the identification of Lynds clouds, Dobashi clouds (named TGU), and high extinction cores (labeled P).

An extinction map of the CMa R1 region based on star counts using the J band data from the near-infrared (near-IR) *DENIS* Catalogue has been performed by Cambr sy (2000). In the region towards the dark clouds the estimated A_J levels are ~ 1 to 4 mag. The maximum extinction provided by the star counting method is a lower limit of $A_J > 6.8$ mag. Adopting the relation between extinctions in optical and infrared bands given by Cardelli et al. (1989), a corresponding visual extinction of $A_V > 24$ mag can be inferred.

Herbst, Racine, & Warner (1978) obtained optical and near-IR photometry as well as spectral types for 30 stars illuminating reflection nebulae in CMa R1. Several of these stars present large V-K colors suggesting a steeper than normal extinction law. Later, Herbst et al. (1982) examined the reddening law applicable to some of these reflection nebulae and verified that the ratio of total to selective extinction is about 4.2. Based on the detection of very large K-L excesses, the presence of circumstellar shells is indicated for two stars (CMa R1-16 and CMa R1-18 in Herbst et al.'s Table I). A similar anomalous extinction was found by Vrba et al. (1987) based upon the wavelength dependence of polarization of stars within CMa R1. The interstellar extinction law towards CMa R1 was also studied by Terranegra et al. (1994). They used *uvby*

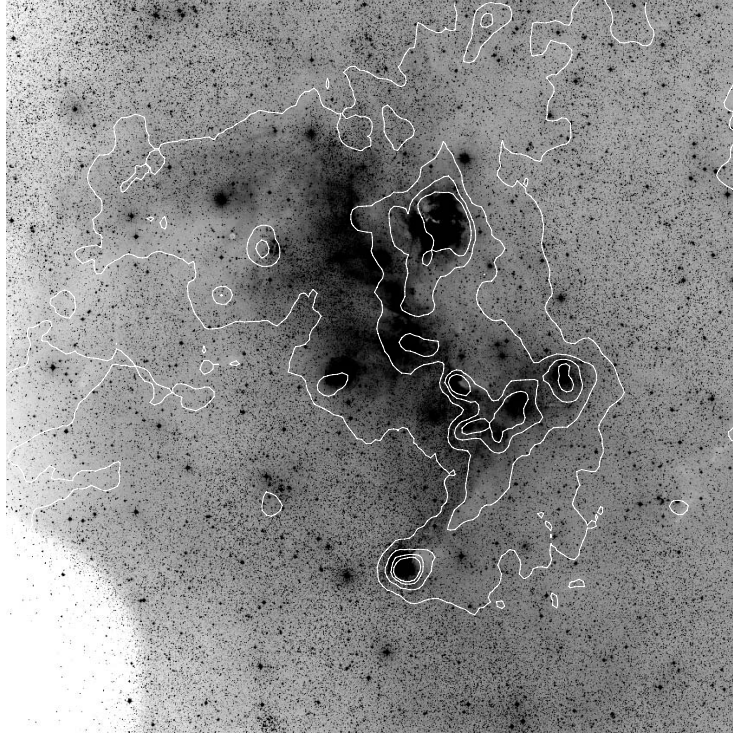


Figure 5. Far-infrared contours superimposed on the optical image of the CMa OB1/R1 region obtained from the Digitized Sky Survey - DSS 2 plate 170. The contours, showing levels 32, 80, 160, and 240 MJy/sr, correspond to IRAS-ISIS data obtained at 100 μ m. Size and orientation are the same as Figure 2.

photometry to derive $R_y = 5.4$ ($R_v = 4.0$) similar to the value estimated by Herbst et al. (1982).

2.2. Gas Distribution

Blitz (1980) has presented a CO map with 10' angular resolution that revealed a molecular emission arising from two distinct clouds. The most intense emission appears to be associated with the HII region S292, and the second cloud seems to be related to S296. A length of 101 pc and a mass of $3 \times 10^4 M_\odot$ were derived for the cloud complex in CMa OB1, based on CO data and adopting a distance of 1.1 kpc.

A more detailed mapping of the region in CO is presented by Machnik et al. (1980), who found 23 peaks of CO emission. A reproduction of this map is shown in Figure 7.

Kim et al. (2004) developed a large scale ^{13}CO survey covering two groups in the CMa OB1 and G 220.8-1.7 (L1656) regions, where they found 22 clouds. The mass spectrum of the clouds shows a power-law with index -1.55 ± 0.09 . A comparative study revealed that the fraction of star-forming clouds is higher among the massive clouds ($M_{\text{cloud}} > 10^{3.5} M_\odot$). Strong UV radiation from O-type stars in the vicinity

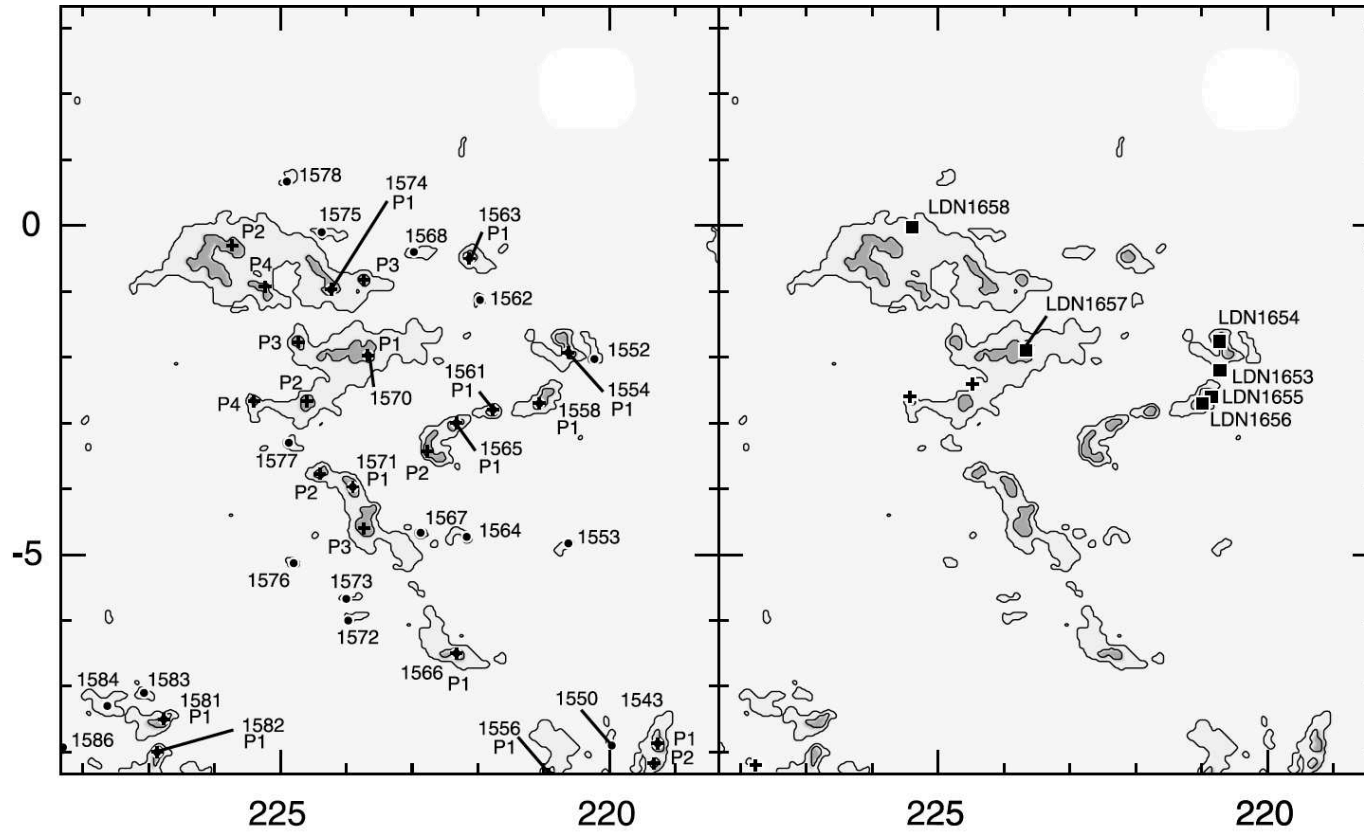


Figure 6 The spatial distribution of the CMa clouds extracted from Dobashi et al. (2005), presented in Galactic coordinates (latitude *versus* longitude). The left panel shows Dobashi et al.'s cloud identifications (TGU). High extinction cores are labeled with “P”. The right side shows the nominal positions from Lynds catalog.

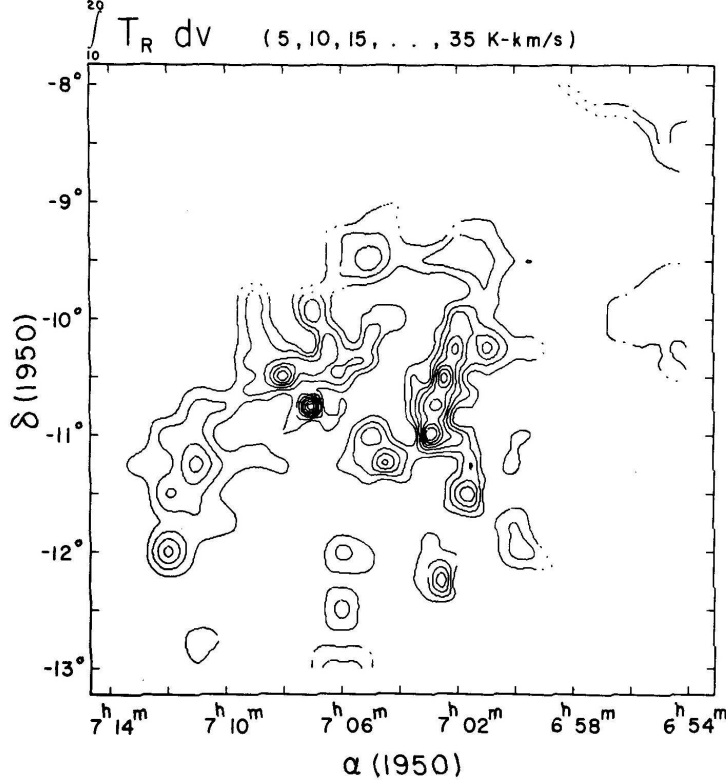


Figure 7. CO map of the central region of CMa OB1, obtained at 2.6 mm. Extracted from Machnik et al. (1980).

of the clouds may explain the small number of low-mass clouds in CMa OB1. Some of the results derived from this survey are presented in Table 2, which lists various objects associated with the ^{13}CO clouds. Figure 8 shows the distribution of the clouds compared with the position of identified objects, as presented by Kim et al. (2004).

Optical absorption line observations of the interstellar CH^+ towards CMa OB1 were reported by Gredel (1997), who found a correlation of $N(\text{CH}^+)$ with the optical depth of the clouds. The results suggest that dissipation of interstellar turbulence is probably the main mechanism of production of CH^+ . Gredel reported CH^+ and CH measurements towards the stars HD 55879, HD 53975, HD 53755, HD 54662, and HD 52382.

A faint, large-scale $\text{H}\alpha$ filament, 80° long and 2° wide, that extends perpendicular to the Galactic plane at $l = 225^\circ$ was discovered by Haffner, Reynolds, & Tufté (1998). This feature appears to meet the Galactic plane above CMa OB1 at $l \sim 225^\circ$, $b \sim 0^\circ$. The radial velocity varies from $v_{\text{LSR}} = +16$ km/s to -20 km/s. The feature seems to have no correspondence to other structures revealed by different wavelength surveys, and the source of ionization was not identified.

Table 2 List of ^{13}CO clouds observed by Kim et al. (2004) towards the CMa region. Cloud name, Galactic coordinates, area and mass of the clouds are given. Last column is used to list the catalogued dark clouds, H II regions, and reflection nebulae.

No.	Cloud name	l ($^{\circ}$)	b ($^{\circ}$)	Area (pc^2)	M_{cloud} (M_{\odot})	Objects associated with the ^{13}CO clouds
1	222.8-00.4	222.80	-0.40	50	1250	
2	223.5-00.9	223.47	-0.93	29	620	S296
3	223.9-01.9	223.87	-1.87	358	16000	L1657, TDS652, S292, S296, vdB93, vdB95
4	224.3-01.1	224.27	-1.07	301	12000	L1658, TDS653, S296
5	224.4-02.4	224.40	-2.40	43	700	TDS654, S296
6	224.4-02.8	224.40	-2.80	14	230	S295, S296, vdB90
7	224.7-02.5	224.67	-2.53	43	890	S296, vdB92
8	224.9+00.8	224.93	0.80	57	640	
9	224.9-01.2	224.93	-1.20	29	720	S296
10	225.3-01.1	225.33	-1.07	43	600	S296
11	225.5-02.8	225.57	-2.80	43	600	S297, S296, vdB94
12	226.1-00.4	226.13	-0.40	315	7500	L1658, S296
13	226.5+01.3	226.53	1.33	57	860	
14	219.7-02.4	219.73	-2.40	?	?	
15	220.4-02.3	220.40	-2.27	22	600	
16	220.8-01.7	220.80	-1.73	87	2200	L1654, BFS62
17	220.9-02.7	220.93	-2.67	70	1700	L1653, L1655, L1656, BFS61, BFS63
18	221.2-02.4	221.20	-2.40	43	1100	BFS63
19	221.5-01.3	221.47	-1.33	38	760	
20	221.6-02.4	221.60	-2.40	27	470	
21	221.7-02.8	221.73	-2.80	32	530	
22	222.4-03.1	222.40	-3.07	22	250	

Notes: Clouds Nos. 1 to 13 are located in the CMa OB1 region, and Nos. 14 to 22 are in the G220.8-1.17 region. The related objects are listed in the following catalogues: dark clouds L (Lynds 1962), and TDS (Taylor et al. 1987); H II regions S (Sharpless 1959), and BSF (Blitz et al. 1982); reflection nebulae vdB (van den Bergh 1966).

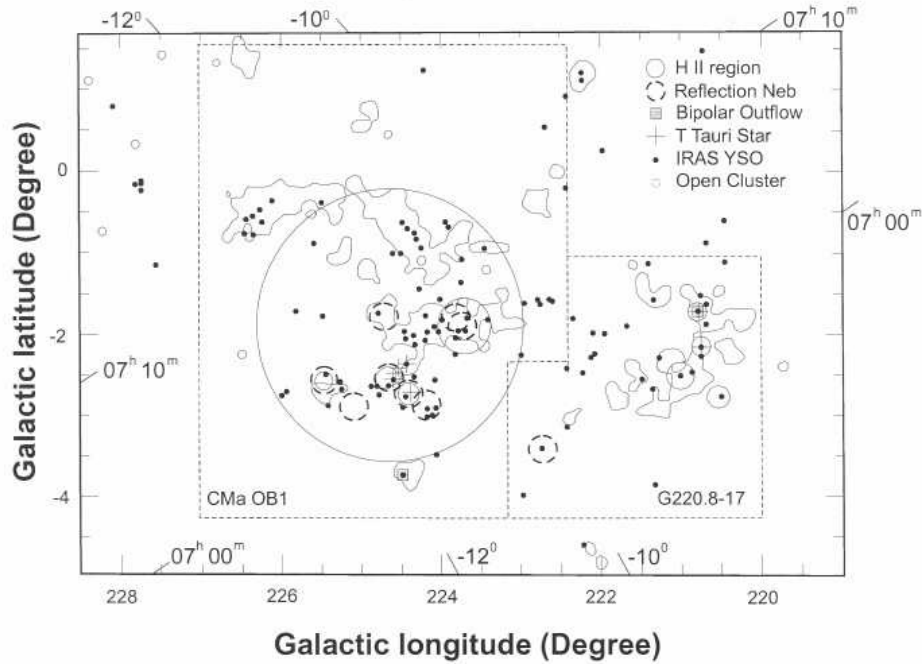


Figure 8. Distribution of CO clouds adapted from Kim et al. (2004). Dotted lines indicate the CMa OB1 and G220.8-1.7 cloud complexes. The boundary of each cloud is indicated by the 1 K km s^{-1} level from the ^{13}CO contour map. Black dots mark YSOs detected by IRAS. A few tick marks are inserted around the margins to indicate the equatorial J2000 coordinates related to the other figures.

2.3. Infrared Emission

The distribution of the mid-IR emission in the CMa OB1/R1 region is shown in Figure 9, an image obtained in the $8.3 \mu\text{m}$ band from the MSX data base. The diffuse emission has a distribution similar to the $100 \mu\text{m}$ map, but more detailed filamentary structures are shown near $(l, b) = (224.2, -2.8)$ and $(223.8, -2)$, for example, corresponding to IC 2177 and GU CMa, respectively.

Luo (1991) used IRAS data to study the infrared emission of the complex CMa OB1/R1 and to compare it to optical, CO and radio continuum observations. The results suggest a composition of diffuse emission and several discrete sources. Two O stars are probably responsible for the diffuse emission which, in combination with the remnant of an old HII region, could produce the extended HII region. Most of the discrete sources have optical counterparts and correspond to the emission or reflection nebulae. The sources which do not have optical counterparts may be excited by early-type stars that are very young and still embedded in dense dust clouds.

The far-IR excess was used as a criterion by Kim et al. (2004) to identify 115 young stellar object candidates, selected from the IRAS point source catalog.

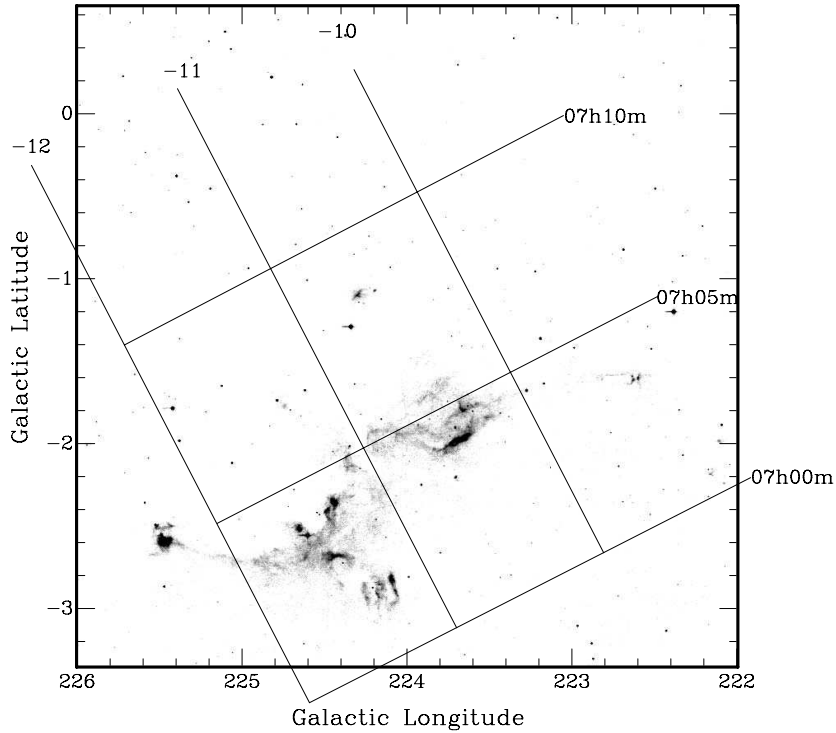


Figure 9. Mid-infrared map of the Canis Major region, obtained by MSX at $8.3 \mu\text{m}$.

3. Stellar Content

Six massive stars are associated with the nebulae around S296. One of them is Z CMa, a young luminous star partly embedded in a dark cloud at the outer edge of S296 (Herbig 1960). Hartmann et al. (1989) classified it as a FU Orionis (FUor) type star. Later, it was discovered that Z CMa is a double system. The primary component is a Herbig Be star and the secondary is a FUor object (Koresko et al. 1991). More details about Z CMa are given in Sect. 3.2. Another interesting object is the unusually bright, variable carbon star W CMa. Assuming that it is a member of the association, and adopting the reddening from the neighboring stars, Eggen (1978) estimated an extreme luminosity for W CMa, $M_{\text{bol}} \sim -7$ mag, similar to the bright carbon stars in the Large Magellanic Cloud.

3.1. Emission Line Stars

Photometric data for large samples of stars located in the CMa OB1 region have been reported by several authors: Feinstein (1967), Eggen (1981), de Geus et al. (1990), and Shevchenko et al. (1999). Herbig & Rao (1974) first identified the emission line stars LkH α 218 (HT CMa) and LkH α 220 (HU CMa). A survey of H α emission line stars made by Wiramihardja et al. (1986) in a $6^\circ \times 7^\circ$ area around CMa OB1 revealed 179 emission line stars, for which *UBV* photometry was carried out.

The detection of new B stars associated with the CMa R1 star forming region was reported by Terranegra et al. (1994). Based on color-magnitude diagrams, four stars were found to be probable new members associated with CMa R1.

Schwartz, Persson, & Hamann (1990) reported the identification of emission-line objects in southern regions. In Canis Major, their study covered a $\sim 2^\circ$ field around $\alpha = 7^h 25^m$, $\delta = -26^\circ$ (J2000), where 26 emission line stars were identified. Based upon spectroscopic data obtained for these objects, Pereira et al. (2001) proposed that 16 of them are Be stars and seven are T Tauri stars.

A more detailed study of the stellar composition of CMa R1 was presented by Shevchenko et al. (1999) in photometric and spectroscopic surveys of 165 stars brighter than V=13 mag, revealing that 88 of them are members of the association. Most of the members are considered pre-main sequence (PMS) stars with ages $< 6 \times 10^6$ yr. Two bright B stars GU CMa and FZ CMa seem to be older than the association and are suggested not to be formed in the same star formation episode. Nine of the CMa R1 members showing circumstellar dust were studied by Tjin A Djie et al. (2001). They suggested that four stars of the sample are Herbig Be stars with disks. The variability of these stars is interpreted in terms of: (i) eclipsing binary (HD 52721); (ii) magnetic activity cycle (HD 53367); or (iii) circumstellar dust variations (LkH α 220 and LkH α 218). The other five stars of the sample, located inside the arc-shaped border of the HII region, do not show indications of circumstellar disks. The absence of a circumstellar disk can be explained by the possible evaporation by UV photons from nearby O stars, or from the nearby supernova that could have occurred about 1 Myr ago.

3.2. Z CMa

The young star Z CMa has been subject to numerous detailed studies. Different spectroscopic and photometric data have been reported: optical spectra obtained by Covino et al. (1984), Finkenzeller & Jankovics (1984), and Finkenzeller & Mundt (1984); ultraviolet spectra by Kenyon et al. (1989); photometric variability investigated by Kolotilov (1991). Long term variability in the optical and near-IR were reported by Covino et al. (1984), Teodorani et al. (1997) and van den Ancker et al. (2004). Zinnecker & Preibisch (1994) detected X-ray emission from the star using *ROSAT* observations, which are detailed in Sect. 6.

Significant spectral changes were discussed by Covino et al. (1984). The FUor nature of Z CMa was first suggested by Hartmann et al. (1989) and confirmed by Hessman et al. (1991) and other authors (Whitney et al. 1993, Torres et al. 1994). Near-IR speckle observations by Leinert & Haas (1987) and Koresko et al. (1989) revealed an elongated emission, with a size of about 0.1 arcsec at $2.2 \mu\text{m}$. The presence of a companion at PA=122 $^\circ$, with separation of 0.1 arcsec, was later confirmed using more detailed near-IR speckle interferometric observations by Koresko et al. (1991) and Haas et al. (1992). Large amounts of cold dust around Z CMa were revealed by sub-

millimeter observations reported by Weintraub et al. (1991). Emission at centimeter wavelengths was also detected by Cohen & Bieging (1986).

A major, well-collimated Herbig-Haro jet, HH 160, emanating from Z CMa was discovered by Poetzel, Mundt, & Ray (1989). The origin of the jet has been the subject of discussion based on polarization studies (Whitney et al. 1993, Fisher et al. 1998, Lamzin et al. 1998). Conflicting results were also obtained using high resolution optical spectroscopy and high angular resolution radio observations. Garcia et al. (1999) identified a microjet associated with the infrared companion, based on speckle interferometry covering the [OI] λ 6300 line of both components with spatial resolution of 0.24 arcsec. The [OI] centroid position is blueshifted in the spectrum of the secondary (the optical object) and redshifted in the primary (near-infrared object), which was interpreted to imply that the primary drives the jet. They also used a deconvolved image of the [OI] emission to show evidence of a microjet whose axis passes through the primary. In contrast, Velázquez & Rodríguez (2001) used sensitive, high resolution VLA observations at 6 cm and 3.5 cm to establish that the jet originates from the optical component. With an astrometric accuracy of 0.002 arcsec, the VLA contour map at 3.5 cm shows the origin of the jet associated with a compact radio source, whose core has an extension to the north-east. Adopting the position of the optical component given by Perryman et al. (1997) and the offsets of the infrared component position by Thiébaud et al. (1995), Velázquez & Rodríguez verified that the core of the radio jet coincides with the optical component. Their conclusions appear to solve the uncertainty on the origin of the jet, which seems to be associated with the secondary (optical) component.

Mader (2001) used AAO/UKST H α wide-field material to search for giant HH flows in CMa OB1/R1 region. Based on these data it is claimed that the HH flow from Z CMa seems to be much larger than previously thought. Chochol et al. (1998) observed large variations on H α , H β , and NaI D P Cygni absorption detected in high-resolution, time resolved data. Several observational facts, mainly related to the variations of the features in multi-component structures, are discussed in terms of wind models of FUor stars. The variations can be explained by equatorial winds and high inclination of the disk.

A new, short outburst of Z CMa was recently reported by van den Ancker et al. (2004), based on the observations of a sudden rise in visual brightness, followed by a rapid decline. This behavior was similar to another eruption that occurred in 1987. Evolutionary calculations show that the system may consist of a $16M_{\odot}$ B0IIf primary star (infrared component) and a $3M_{\odot}$ FUor secondary (optical component), with a common age of about 3×10^5 yrs. The strength of emission lines originating from the envelope of the primary star showed strong increase with the brightness, which can be interpreted in terms of an accretion disk with atmosphere associated with the Herbig Be component.

Both sources were observed by the Keck interferometer in the K band. The FUor object was discussed by Millan-Gabet et al. (2006), who verified that spatial scales of near-infrared emission are large compared to the predictions from simple models of accretion disks. They suggested that disk models require modifications or that additional model components are required. A definitive analysis of the data was not possible for the Herbig Ae component (Monnier et al. 2005). Schütz, Meeus, & Sterzik (2005) obtained N-band photometry and spectroscopy for the FUor component, which showed a broad absorption band attributed to silicates. Polonski et al. (2005) published high spatial resolution mid-IR imaging and spectroscopy, sub-millimeter photometry, and 3-4 μ m photometry. A simple radiative transfer model was adopted to fit the mid-IR

observed spectra to derive a dust temperature of $T=274$ K and the sub-millimeter flux was used to derive a dust mass of $8 \times 10^{-3} M_{\odot}$.

4. Clusters

The relation between CMa OB1 and the open clusters NGC 2353, 2343 and 2335 was discussed by Clariá (1974b) based on a comparison of their distances and ages. The conclusion of this study was that NGC 2353 seems to be the nucleus of CMa OB1, as proposed by Ruprecht (1966). The physical connection of the OB association with CMa R1 and NGC 2353 was also supported by Herbst, Racine & Warner (1978) and by Eggen (1978). However, this was contradicted by the detailed study of Fitzgerald et al. (1990), see Sect. 1. Also, NGC 2343 and 2335 have ages of about 10^8 yrs, which indicates they were formed before the association and are not related to it.

As mentioned in Sect. 1, the relation between the cluster Cr 121 and CMa OB1 was discussed by Eggen (1981), suggesting the separation of two groups of stars in this direction: Cr 121 is considered a compact open cluster located at the same distance as CMa OB1, and NGC 2287, a more diffuse group, forms a nearer association, suggested to be CMa OB2. More recently, de Zeeuw et al. (1999) studied the structure and the evolution of nearby young clusters, based on *Hipparcos* data. Astrometric members were identified in young stellar groups out to a distance of ~ 650 pc. A moving group in the CMa OB1/R1 region could not be identified because the candidate members have small proper motions and parallaxes. In the direction of Cr 121, de Zeeuw et al. selected 103 stars, for which a mean distance of 592 ± 28 pc was derived. The proper motions for 43 stars that were previously considered Cr 121 members (Collinder 1931; Schmidt-Kaler 1961; Feinstein 1967; Eggen 1981) were analysed by de Zeeuw et al. to reveal evidence for a moving group, but 25 of the 43 stars were rejected by their selection procedure. Based on the differences of the mean proper motions, de Zeeuw et al. claim that Eggen's proposed division in two groups is unphysical. However, the fact that *Hipparcos* parallaxes are unreliable at large distances must be considered, indicating that these data could only detect the more diffuse foreground association. The same biased selection method was used by Dias et al. (2001) to classify as Cr 121 members only the nearer stars of the field, and to determine a distance of 470 pc and an age of 11 Myr for this group of stars (Dias et al. 2002). Burningham et al. (2003) studied the low mass PMS stars discovered by *XMM-Newton* and *ROSAT* observations towards Cr 121. Their results are not in agreement with the scenario proposed by de Zeeuw et al., in which these low-mass stars are associated with the nearer moving group suggested to be Cr 121. Burningham et al. argue that the PMS stars are associated with a young cluster located at 1050 pc. They confirm that the moving group detected by de Zeeuw et al. is a foreground association and should be called CMa OB2, in agreement with Eggen's proposition. Kaltcheva (2000) also suggested the separation of two groups: Cr 121 is a more compact cluster at 1085 pc, and the other group of stars lies at 660 - 730 pc, having characteristics of an OB association. More recent results were obtained by Kaltcheva & Makarov (2007) using corrected *Hipparcos* parallaxes, which indicated a distance of 750-1000 pc for Cr 121, in agreement with the previous results based on photometric parallaxes.

Soares & Bica (2002) used JHK data from the 2MASS Catalogue to study embedded star clusters associated with NGC 2327 and BRC 27 which is a bright-rimmed cloud (Sugitani et al. 1991) at $\alpha_{J2000} = 7^h04^m$, $\delta_{J2000} = -11^{\circ}23'$. Based on color-

magnitude diagrams they derived a distance of ~ 1.2 kpc for both clusters, and estimated similar ages of about 1.5 Myr. The mean visual extinction in the direction of the objects were estimated to be $A_V = 5.5$ in NGC 2327 and $A_V = 6.5$ in BRC 27. A subsequent paper (Soares & Bica 2003) presented the study of two other clusters in the nebulae vdB 92 (van den Bergh 1966) and Gy 3-7 (Gyulbudaghian 1984). They adopted the kinematic distance of 1.41 kpc for Gy 3-7 (Wouterloot & Brand 1989), while the distance estimated for vdB 92 is 1.5 ± 0.3 kpc. According to their results, the age derived for vdB 92 is 5-7 Myr and for Gy 3-7 is ~ 2 Myr. The mean visual extinctions are $A_V = 4.4$ and $A_V = 6.3$ mag, respectively.

5. Distance

The first determinations of the distance to the CMa OB association were quite uncertain mainly due to the lack of completeness of the member content.

Racine (1968) reported photometric and spectroscopic observations of the CMa R1 members listed by van den Bergh (1966). The data were used to determine a mean distance of 690 ± 120 pc. Clariá (1974a) used a color-magnitude diagram based on the early-type stars in the CMa OB1 region to estimate a distance of 1150 ± 140 pc for the association. A more detailed study (Clariá 1974b) was based on photometric and spectroscopic data of 44 stars, selected as members or probable members of CMa R1. Clariá noted that most of the stars studied by Racine in CMa R1 were shown to be CMa OB1 members and compared the distance moduli that he obtained with those values estimated by Racine (1968). He argues that the discrepancies are due to differences in the adopted MK types and/or to the disagreement between the absolute magnitude derived from different hydrogen lines. By correcting these differences and considering only the true members of CMa R1 (those which are CMa OB1 members) the derived distance is 1050 ± 170 pc.

Tovmassian et al. (1993) observed 43 early-type stars of the OB association in CMa and they concluded that these stars compose 3 groups situated at distances 320, 570 and 1100 pc. Later, Shevchenko et al. (1999) derived a distance of 1050 ± 150 pc based on photometry of 88 early-type stars that were found to be probable members of the CMa R1.

The distribution of young stellar groups in Canis Major was studied and updated by Kaltcheva & Hilditch (2000) using $uvby\beta$ photometry of intrinsically luminous OB stars ($V < 9.5$ mag). They confirmed a distance of 990 ± 50 pc for CMa OB1, suggesting an overestimation of the spectroscopic distances used in the previous studies.

Considering the various estimates, it seems reasonable to recommend the use of 1000 pc for the distance of the CMa clouds.

6. X-ray Emission

In order to search for PMS stars, T. Montmerle and collaborators have studied *ROSAT* images of moderately distant molecular clouds. Most of the selected sources show properties of low- and intermediate-mass PMS stars: point-like sources are T Tauri and Herbig Ae/Be stars, while extended emission seems to be due to unresolved young stellar clusters (Gregorio-Hetem et al. 1998). The 20 ksec *ROSAT* PSPC image obtained for the CMa R1 region revealed 47 sources in the central region of the field,

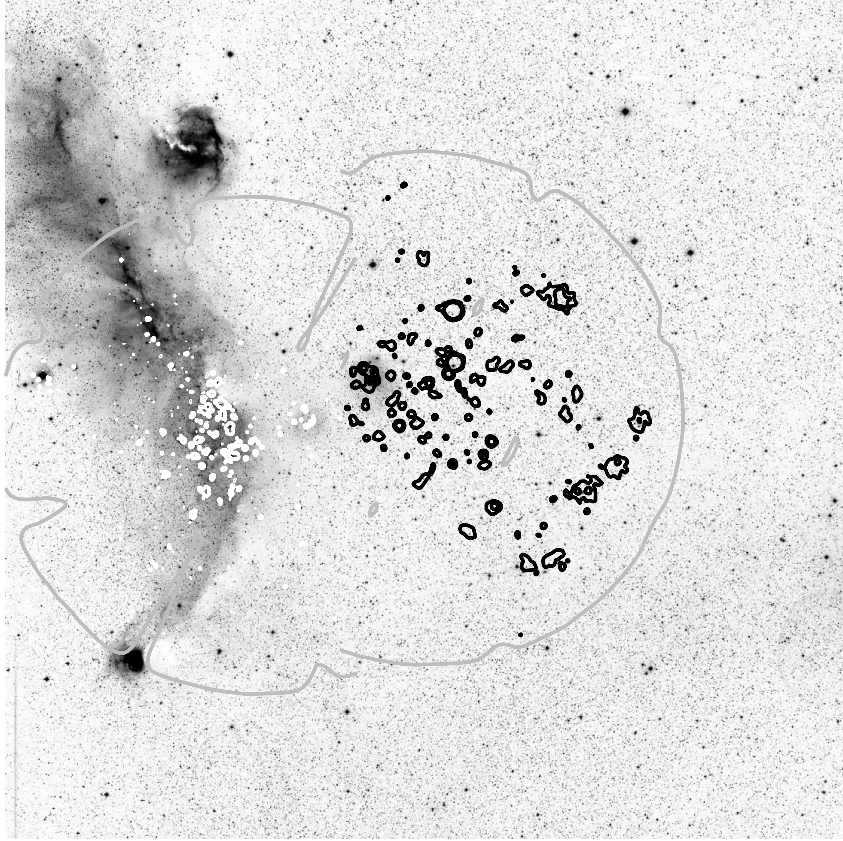


Figure 10. Optical POSS (R) image obtained from a digitized POSS (R) plate made with the *Machine Automatique à mesurer pour l'Astronomie* (MAMA) micro-densitometer at Observatoire de Paris superimposed with X-ray contours obtained from two ROSAT images covering the CMA R1 region. The sources indicated by white contours (east field) are described by Zinnecker & Preibisch (1994), and the sources in black contours (west field) by Gregorio-Hetem, Montmerle, & Marciotto (2003). The image is 3×3 square degrees. North is up and East is to the left.

with $\sim 80\%$ having at least one optical counterpart. Several optical counterparts are emission-line stars classified as members of CMA R1 (Shevchenko et al. 1999). The bolometric luminosity and spectral type for these optical counterparts indicate that most of them have $\log(L_X/L_{bol})$ in the -6 to -4 range. The 2MASS Catalogue was used to search for sources coincident with the *ROSAT* position error circles, revealing at least one near-IR counterpart candidate for 90% of the X-ray sources. In several cases, multiple candidates were related to a single extended X-ray emission, possibly corresponding to embedded clusters. The evaluation of the color-magnitude (J-H vs. J) indicates that 55% of the sample is consistent with a low-mass young population, 37% are intermediate-mass stars and 8% are massive stars (Gregorio-Hetem, Montmerle, &

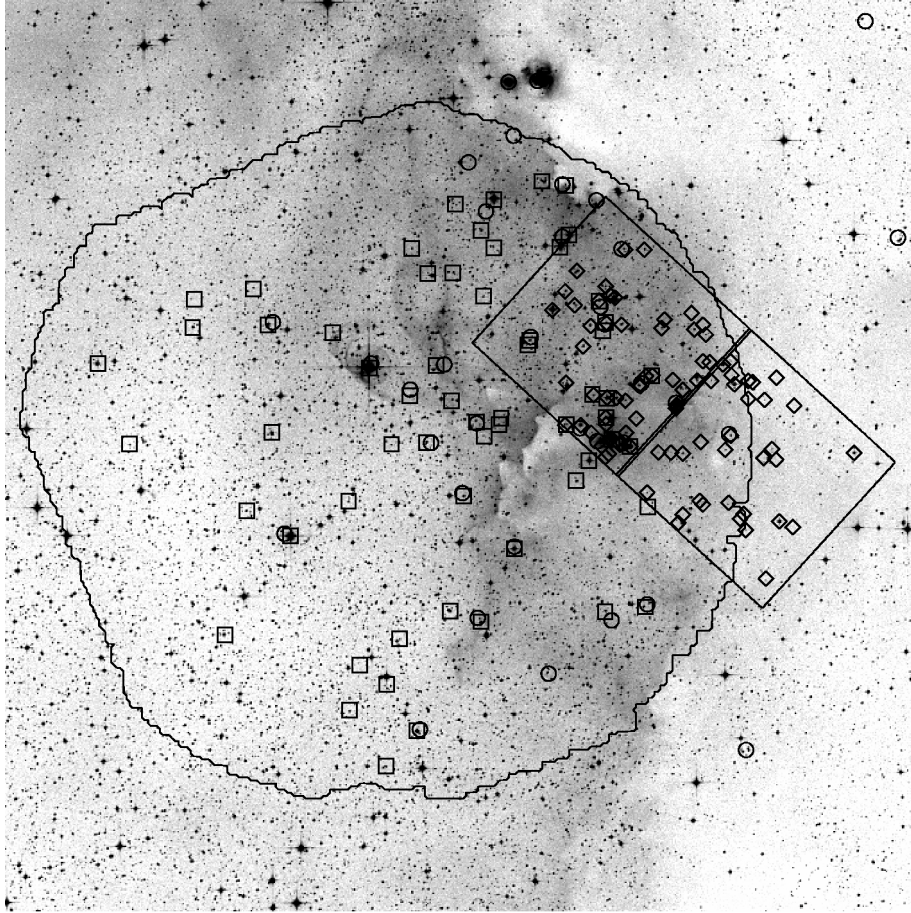


Figure 11. Recent X-ray observations in CMa R1: the large round area corresponds to the XMM-Newton field of view, and the two squares at the right indicate the location of Chandra ACIS-S observations. Open small squares, diamonds and circles show respectively XMM, Chandra and ROSAT detected sources (extracted from Rojas et al. 2006).

Marciotto 2003). Additional optical counterparts were identified based on Gemini VRI data of five X-ray sources in CMa R1. Several counterpart candidates were found to be associated with each source, showing optical and near-infrared colors typical of young stars (Gregorio-Hetem, Rodrigues, & Montmerle 2007).

An extended feature is also present in the eastern part of the field, the nature of which is unclear from these *ROSAT* data: it could be an unresolved stellar cluster, since the point spread function of the PSPC is very degraded towards the edge of the field; or a truly diffuse emission, since it is very precisely located on top of an optical diffuse feature, which is argued to be either a “fossil” HII region, or an old SNR.

Zinnecker & Preibisch (1994) performed a PSPC survey of X-ray emission from Herbig Ae/Be stars in this region, but found no evidence for extended emission, perhaps due to their short exposures (~ 5 ksec). This survey revealed a X-ray luminosity of $(1.4 \pm 0.7) \times 10^{31}$ erg/s for Z CMa, but could not detect GU CMa. Figure 10 is a

composite of both *ROSAT* images obtained of CMa R1. The field covering the eastern part is described by Zinnecker & Preibisch (1994), and the western part by Gregorio-Hetem, Montmerle, & Marciotto (2003). The extended feature mentioned above is not visible in Figure 10, since it was overlapped by the image obtained by Zinnecker & Preibisch (1994).

Improved X-ray observations of the CMa R1 region were recently performed with the XMM-Newton telescope towards a 30' field of view around the extended emission detected by *ROSAT*, aiming to elucidate its origin and to distinguish between unresolved sources and diffuse emission (Gregorio-Hetem et al. 2008). The new data set reveals the presence of 61 X-ray sources within the observed field, spatially distributed in clusters previously unresolved. The XMM data answer the question on the nature of the extended emission, which appears to be due to unresolved sources, and seems not to be related to diffuse X-ray emission. An area of 17×17 arcmin² in the outer edge of S296 was covered by Chandra, revealing several additional faint sources in the field. Using the abovementioned XMM-Newton observations, supplemented with Chandra archival data, Rojas et al. (2006) identified a total of 135 X-ray sources in the CMa region, see Figure 11. The correlation of near-IR counterparts with these X-ray sources indicates that they are probably young stars.

7. Star Formation induced by a SNR?

Herbst & Assousa (1977) reported evidence for star formation in CMa R1 induced by a supernova explosion. The suggestion is based on: (i) the form of a large scale ring of emission nebulosity with a diameter of about 3°, defined by S296 and fainter nebulae to the north and east, which could be an old supernova remnant; (ii) the absence of luminous stars at the ring center, which is confirmed by the far ultraviolet image of the field by Henry (1988); (iii) an expanding neutral hydrogen shell coinciding with the optical feature and evident in the H I maps of Weaver & Williams (1974); (iv) the discovery in CMa OB1 of a runaway star, HD 54662, that could be associated with the event that produced the SNR. Velocity information for the components of the CMa OB1/R1 complex was compiled by Herbst & Assousa (1977) from different catalogues of H I, Ca II, CO and H II velocities to estimate the mean radial velocity of the association. They verified that the early-type star HD 54662 lies within the ring, but it is offcenter and has a radial velocity differing by about 30 km/s from the velocity inferred for the association. Based on its peculiar velocity, HD 54662 was considered a possible runaway star, but confirmation depends on an accurate determination of the proper motion.

Herbst & Assousa (1977) compared the SNR properties with models of SNRs evolving in a uniform medium to derive an age of 5×10^5 yrs for the supernova shell. A study of the optical and infrared properties of the stars in CMa R1 by Herbst, Racine, & Warner (1978) provided an estimate of a similar age for most of the members of the R association, compatible with the suggestion of star formation triggered by a supernova in this region. On the other hand, Shevchenko et al. (1999) concluded that only a minor fraction of the young stars in CMa R1 could have been created by the mechanism suggested by Herbst & Assousa, since the majority of them have ages that are much older than that required by this scenario.

Radio-continuum observations obtained by Nakano et al. (1984) indicate that the OB stars are sufficient to ionize the emission nebulosity. The number of Lyman continuum photons emitted by seven of the brightest members (HD 54662, 53975, 53974,

53367, 54879, 53456, 53755) was computed to determine the total photon flux from OB stars. The comparison with the thermal spectrum exhibited by S296 confirms the ionization balance between OB stars and the ionized gas in this region. A SNR could have produced the ring morphology and triggered the episode of star formation, but the remnant would be so old that no trace of non-thermal emission would be expected today.

Vrba et al. (1987) performed a linear polarization survey in the direction of CMa R1 in order to test the hypothesis of star formation driven by a shock wave. The polarizations were found to be inconsistent with a scenario of quiescent cloud collapse. These results are compatible with a simple model of the compression by a supernova-induced spherical shock front of an initially uniform interstellar magnetic field, or alternatively, the shell-like structure could be produced by stellar winds.

The gas velocities in the region were also estimated by Reynolds & Ogden (1978) measuring the $H\alpha$, [NII] and [OIII] lines, which were used to confirm that the large shell is in expansion with a velocity of about 13 km/s. The authors also noted that the ultraviolet fluxes of two hot stars, HD 54662 and HD 53975, located within the ring are sufficient to account for the temperature and ionization of the shell. Based on these results, Reynolds & Ogden suggested strong stellar winds, or an evolving HII region, as alternatives to the SNR hypothesis, as also suggested by Blitz (1980) and Pyatunina & Taraskin (1986).

More recently, Comerón et al. (1998) used proper motions measured by *Hipparcos* to reveal a clearly organized expanding pattern in CMa OB1 showing LSR velocity of ~ 15 km/s. Their results on the magnitude and spatial arrangement of the expanding motions suggest that very energetic phenomena are responsible for the formation of the OB association. A rough determination of the center at $(l, b) = (226.5, -1.6)$ and age ~ 1.5 Myr was carried out for the expanding structure. A new runaway star HD 57682 was discovered, showing a motion directly away from the derived center of expansion, which supports the scenario suggested by Herbst & Assousa.

Acknowledgements. This chapter is based on the original work “The Canis Majoris OB1 Associations” published by George Herbig 15 years ago in the ESO book “Low Mass Star Formation in Southern Molecular Clouds”. I would like to express my gratitude to Dr. Herbig for his kindness to provide some of the original figures and for his valuable comments on the manuscript. A special thank goes to Bo Reipurth for his suggestions and for critiquing drafts of the manuscript. I also thank Mario van den Ancker, the referee, for constructive comments that improved the presentation of the chapter; John P. Gleason for kindly providing Figure 1; and Steve Rodney for useful suggestions on the layout of tables.

This work has made use of the SIMBAD, VizieR, and Aladin databases operated at CDS, Strasbourg, France. Partial financial support from FAPESP (Procs. No. 2001/09018-2 and No. 2005/00397-1) is also acknowledged.

References

- Ambartsumian, V. A. 1947, in *Stellar Evolution and Astrophysics*, Armenian Acad. of Sci. (German transl., 1951, Abhandl. Sowjetischen Astron., 1, 33)
- Becker, W. 1963, *Zeitschrift f. Astrophys.*, 57, 117
- Blitz, L. 1980, in *Giant molecular Clouds in the Galaxy*, eds. M. G. Edmunds and P.M. Solomon, p. 211

- Blitz, L., Fich, M., & Stark, A. A. 1982, ApJS, 49, 183
- Burningham, B., Naylor, T., Jeffries, R. D., & Devey, C. R. 2003, MNRAS, 346, 1143
- Cambr  sy, L. 2000 (private communication)
- Cardelli, J.A., Clayton, G.C., & Mathis, J.S. 1989, ApJ, 345, 245
- Chochol, D., Teodorani, M., Strafella, F., Errico, L. & Vittone, A. A. 1998, MNRAS, 293, L73
- Clari  , J.J. 1974a, AJ, 79, 1022
- Clari  , J.J. 1974b, A&A, 37, 229
- Cohen, M. & Bieging, J. H. 1986, AJ, 89, 1868
- Collinder, P. 1931, Annals Obs. Lund, 2, 1
- Comer  n, F., Torra, J., & Gomez, A. E. 1998, A&A, 330, 975
- Covino, E., Terranegra, L., Vittone, A. A., & Russo, G. 1984, in *Physics of Formation of Fe II lines Outside LTE*, eds. R. Viotti et al., Reidel, p. 143
- de Geus, E. J., Lub, J., & van de Grift, E. 1990, A&AS, 85, 915
- de Zeeuw, P. T., Hoogerwerf, R., & de Bruijne, J. H. J. 1999, AJ, 117, 354
- Dias, W. S., L  pine, J. R. D., & Alessi, B. S. 2001, A&A, 376, 441
- Dias, W. S., Alessi, B. S., Moitinho, A., & L  pine, J. R. D. 2002, A&A, 389, 871
- Dobashi, K., Uehara, H., Kandori, R., Sakurai, T., Kaiden, M., Umemoto, T., & Sato, F. 2005, PASJ, 57, S1
- Eggen, O. J. 1978, PASP, 90, 436
- Eggen, O. J. 1981, ApJ, 247, 507
- Feinstein, A. 1967, ApJ, 149, 107
- Finkenzeller, U. & Jankovics, I. 1984, A&AS, 57, 285
- Finkenzeller, U. & Mundt, R. 1984, A&AS, 55, 109
- Fischer, O., Stecklum, B., & Leinert, Ch. 1998, A&A, 334, 969
- Fitzgerald, M. P., Harris, G. L. H., & Reed, B. C. 1990, PASP, 102, 865
- Garcia, P. J. V., Thi  baut, E., Bacon, R. 1999, A&A, 346, 892
- Gredel, R. 1997, A&A, 320, 929
- Gregorio-Hetem, J., Montmerle, T., Casanova, S., & Feigelson, E. D. 1998, A&A, 331, 193
- Gregorio-Hetem, J., Montmerle, T., & Marciotto, E. 2003, in *Open Issues in Local Star Formation*, eds. J. L  pine & J. Gregorio-Hetem, Kluwer, p. 193
- Gregorio-Hetem, J., Rodrigues, C. V., & Montmerle, T. 2007, in *Triggered Star Formation in a Turbulent ISM*, eds. B. G. Elmegreen & J. Palous, IAU Symposium 237, Cambridge University Press, p.414
- Gregorio-Hetem, J., Rojas, G., Montmerle, & Grosso, N. 2008, in preparation.
- Gyulbudaghian, A. L. 1984, Astrofizika, 20, 631
- Haffner, L. M.; Reynolds, R. J., & Tufte, S. L. 1998, ApJ, 501, L83
- Hartmann, L., Kenyon, S. J., Hewett, R., Edwards, S., Strom, K. M., Strom, S. E., & Stauffer, J. R. 1989, ApJ, 338, 1001
- Haas, M., Christou, J., Zinnecker, H., Ridgway, S., & Leinert, C. 1993, A&A 269, 282
- Henry, R. C. 1988, *Atlas of the Ultraviolet Sky* (Baltimore: Johns Hopkins Univ. Press)
- Herbig, G. H. 1960, ApJS, 4, 337
- Herbig, G.H. 1991, in ESO Scientific Report No.11 *Low Mass Star Formation in Southern Molecular Clouds*, Ed. Bo Reipurth, p.233
- Herbig, G.H. & Rao, N.K., 1972, ApJ, 174, 401
- Herbst, W. & Assousa, G.E. 1977, ApJ, 217, 473
- Herbst, W., Miller, D.P, Warner, J.W., & Herzog, A. 1982, AJ, 87, 98
- Herbst, W., Racine, R., & Warner, J.W. 1978, ApJ, 223, 471
- Hessman, F. V., Eisl  ffel, J., Mundt, R., Hartmann, L. W., Herbst, W., & Krautter, J. 1991, ApJ, 370, 384
- Hoag, A. A., Johnson, H. L., Iriarte, B., Mitchell, R. I., Hallam, K. L., & Sharpless, S. 1961, Publ. US Naval Obs., 17, 345
- Kaltcheva, N. T. 2000, MNRAS, 318, 1023
- Kaltcheva, N. T. & Hilditch, R.W. 2000, MNRAS, 312, 753
- Kaltcheva, N. T. & Makarov, V., 2007, ApJ, 667, 155
- Kenyon, S. J., Hartmann, L. W., Imhoff, C. L., & Cassatella, A. 1989, ApJ, 334, 925

- Kim, B. G., Kawamura, A., Yonekura, Y., & Fukui, Y. 2004, PASJ, 56, 313
- Kolotilov, E. A. 1991, Soviet Astron. Lett., 17, 144
- Kopylov, I. M. 1958, Soviet Astron., 2, 359
- Koresko, C. D., Beckwith, S. V. W., & Sargent, A. I. 1989, AJ, 98, 1394
- Koresko, C. D., Beckwith, S. V. W., Ghez, A. M., Matthews, K., & Neugebauer, G. 1991, AJ, 102, 2073
- Lamzin, S. A., Teodorani, M., Errico, L., Vittone, A. A., Kolotilov, E. A., Miroshnichenko, A. S., & Yudin, R. V. 1998, Ap&SS, 261, 161
- Leinert, Ch. & Haas, M. 1987, A&A 182, L47
- Luo, S-G. 1992, Chinese Astronomy and Astrophysics, 16, 33
- Lynds, B. T. 1962, ApJS, 7, 1
- Mader, S. L. 2001, PhD Thesis University of Wollongong, Australia
- Machnik, D. E., Hettrick, M. C., Kutner, M. L., Dickman, R. L., & Tucker, K. D. 1980, ApJ, 242, 121
- Markarian, B. E. 1952, *Proc. Acad. Sci. Armenian SSR* 15, 13
- Millan-Gabet, R., Monnier, J. D., Akenson, R. L., Hartmann, L., Berger, J. P. et al. 2006, ApJ 641, 547
- Monnier, J. D., Millan-Gabet, R., Billmeier, R., Akenson, R. L., Wallace, D. et al. 2005, ApJ 624, 832
- Nakano, M., Yoshida, S., & Kogure, T. 1984, PASJ 36, 517
- Pereira, C. B., Schiavon, R. P., de Arajo, F. X., Landaberry, S. J. C. 2001 AJ, 121, 1071
- Perryman, M. A. C., Lindegren, L., Kovalevsky, J. et al. 1997, A&A, 323, L49
- Poetzel, R., Mundt, R., & Ray, T. P. 1989, A&A, 224, L13
- Polomski, E. F.; Woodward, C. E., Holmes, E. K.; Butner, H. M.; Lynch, D. K., Russell, R. W., Sitko, M. L., Wooden, D. H., Telesco, C. M., & Piña, R. 2005, AJ, 129, 1035
- Pyatunina, T. B. & Taraskin, Yu. M. 1986, Astron. Zhurnal, 63, 1098
- Racine, R. 1968, AJ, 73, 233
- Reynolds, R. J. & Ogden, P. M. 1978, ApJ, 224, 94
- Rojas, G., Gregorio-Hetem, J., Montmerle, & Grosso, N. 2006, in ESA SP-604, Proceedings of *The X-ray Universe 2005*, El Escorial, Madrid, Spain, 107
- Ruprecht, J. 1966, IAU Trans., 12B, 348
- Sharpless, S. 1959, ApJS, 4, 257
- Shevchenko, V. S., Ezhkova, O. V., Ibrahimov, M. A., van den Ancker, M. E., & Tjin A Djie, H. R. E. 1999, MNRAS, 310, 210
- Schmidt-Kaler, T. 1961, Z. Astrophys. 53, 28
- Schütz, O., Meeus, G., & Sterzik, M. F. 2005, A&A, 431, 165
- Soares, J. B. & Bica, E. 2002, A&A, 388, 172
- Soares, J. B. & Bica, E. 2003, A&A, 404, 217
- Sugitani, K., Fukui, Y., & Ogura, K. 1991, ApJS, 77, 59
- Schwartz, R. D., Persson, S. E., Hamann, F. W. 1990 AJ, 100, 793
- Taylor, D. K., Dickman, R. L., & Scoville, N. Z. 1987, ApJ, 315, 104
- Teodorani, M., Errico, L., Vittone, A. A., Giovanelli, F., & Rossi, C. 1997, A&AS, 126, 91
- Terranegra, L., Chavarria-K., C., Diaz, S., & Gonzalez-Patino, D. 1994, A&A, 104, 557
- Thiebaud, E., Bouvier, J., Blazit, A., Bonneau, D., Foy, F. -C., & Foy, R. 1995, A&A, 303, 795
- Tjin A Djie, H. R. E., van den Ancker, M. E., Blondel, P. F. C., Shevchenko, V. S., Ezhkova, O. V., de Winter, D., & Grankin, K. N. 2001, MNRAS, 325, 1441
- Torres, C. A. O., Quast, G. R., de la Reza, R., Lépine, J. R. D., & Gregorio-Hetem, J. 1994, AJ, 109, 2146
- Tovmasyan, H. M., Oganesyan, R. Kh., Epremian, R. A., & Yugenien, D. 1993, AZh, 70, 451
- van den Ancker, M. E., Blondel, P. F. C., Tjin A Djie, H. R. E., Grankin, K. N., Ezhkova, O. V., Shevchenko, V. S., Guenther, E., & Acke, B. 2004, MNRAS, 349, 1516
- van den Bergh, S. 1966, AJ, 71, 990
- Velázquez, P. F. & Rodríguez, L. F. 2001, Rev. Mex. Astron. Astrofis., 37, 261
- Vrba, F. J., Baierlein, R., & Herbst, W. 1987, ApJ, 317, 207
- Weaver, H. & Williams, D. R. W. 1974, A&AS, 17, 1

- Weintraub, D. A., Sandell, G., & Duncan, W. 1991, ApJ, 382, 270
- Whitney, B. A., Clayton, G. C., Schulte-Ladbeck, R. E., Calvet, N., Hartmann, L., & Kenyon, S. J. 1993, ApJ, 417, 687
- Wiramihardja, S.D., Kogure, T., Nakano, M., & Yoshida, S. 1986, PASJ, 38, 395
- Wouterloot, J. G. A., & Brand, J. 1989, A&AS, 80, 149
- Zinnecker, H. & Preibisch, T. 1994, A&A, 292, 152